Surface Review and Letters, Vol. 4, No. 6 (1997) 1161–1165

NUCLEATION AND GROWTH OF Cu/Ni(100): A VARIABLE TEMPERATURE STM STUDY

B. MÜLLER, L. NEDELMANN, B. FISCHER, H. BRUNE and K. KERN
Institut de Physique Expérimentale, Ecole Polytechnique Fédérale de Lausanne, CH-1015 Lausanne, Switzerland

A detailed study of the nucleation and growth of Cu on Ni(100) as a function of substrate temperature and deposition rate by variable temperature STM is reported. By the quantitative analysis of the saturation island density as a function of temperature and flux for submonolayer coverages, we have deduced the migration barrier (0.35 eV), the dimer bond energy (0.46 eV) as well the sizes of the the critical nuclei. Because the dimer bond energy is large with respect to the migration barrier, a well-defined transition from a critical nucleus of 1 to 3 has been observed, as expected from the adsorption site geometry on square lattices. The large dimer bond energy of Cu on Ni(100) is one of the physical reasons for the recently uncovered strain relief mechanism via internal {111} faceting. The substantially increased island density on mono- and bilayer copper films on Ni(100) with respect to multilayer films might also be attributed to the enhanced lateral bonding.

The fundamental processes in epitaxial growth of thin films by molecular beam epitaxy (MBE) involve nucleation, growth and coalescence of islands. The distribution of the island sizes, their density and shape are closely related to the external parameters substrate temperature and flux. In particular, a quantitative analysis of the variation of the saturation island density with substrate temperature and deposition rate can be used to extract microscopic parameters such as the activation barrier for surface migration by application of mean field nucleation theory.[1] Recently, the validity of nucleation theory has been experimentally proven for fcc(111) metal surfaces.[2] *A priori*, nucleation theory should also be applicable to epitaxial growth on surfaces with different symmetry. In the paper we present results of Cu nucleation on Ni(100), a substrate with square symmetry, and show that the difference in bond geometry leads to features characteristic for this symmetry. An important physical quantity in nucleation is the critical nucleus. It refers to the island size i containing one atom less than the number of atoms needed to create the smallest stable island. Here, "stable" refers to the time scale of deposition, i.e. stable islands have a higher probability to grow than to dissociate during deposition. For very low temperatures, for example, one may find that the monomers do not migrate at all (statistical growth, $i = 0$). By increasing the temperature the situation changes, the monomers can migrate, but the dimer is stable ($i = 1$). Increasing the temperature further, the trimer ($i = 2$), tetramer ($i = 3$) and so on might become the smallest stable island. This classic continuum model ignores the adsorption site geometry of the substrate, which does indeed not matter for the critical island sizes $i = 0$ and $i = 1$. The adsorption site geometry becomes, however, important on square lattices when $i = 2$. The dissociation of both dimers ($i = 1$) and trimers ($i = 2$) is characterized by single bond breaking and therefore associated with similar dissociation energies. Hence, on square lattices, one expects a direct transition from $i = 1$ to $i = 3$. Above $i = 3$, there is no well-defined behavior since all islands on square lattices are characterized by single or double bond breaking. Thus, on square lattices the "magic" islands are expected to be the dimer and the tetramer.[3]

The growth of copper on Ni(100) has been investigated by a variable temperature STM between 100 and 400 K; analogous instrumentation as used here is described in Ref. 4. The nickel crystal was prepared by argon ion sputtering and subsequent annealing to 1200 K resulting in nearly perfect terraces of several hundred nanometers. Copper was deposited by

thermal evaporation from a Knudsen type MBE source at a background pressure better than 5×10^{-10} mbar. The growth rate has been calibrated from STM images with monolayer coverage. The STM measurements have been performed in the constant current mode at 0.5–2.0 V positive or negative bias and 0.5–8.0 nA tunneling current.

Figure 1 shows two typical STM images characterizing the variation of the saturation island density as a function of substrate temperature. Low substrate temperatures result in high island densities; higher substrate temperatures give considerably lower island densities for a fixed deposition rate. These island densities directly reflect the adatom mobility, which depends exponentially on substrate temperature. The island density was determined by counting the islands and dividing by the area of the image. The size of the analyzed area has been corrected for thermal drift by determination of characteristic features at successively obtained images. The influence of structural defects such as steps is excluded since we have depicted areas far away from such defects. This is a major advantage of STM with respect to integral methods like electron diffraction.

If the saturation island density is determined as a function of substrate temperature and deposition rate, the microscopic material parameters migration barrier E_m, dimer bond energy E_b and attempt frequency v_0 can be obtained using nucleation theory.[1,2] Copper is known to grow on Ni(100) in the layer-by-layer mode (see also below), and re-evaporation of copper atoms from the surface can be neglected in the considered temperature range (100–400 K). On this basis, the saturation island density n_x is only a function of deposition rate R and substrate temperature T and given for a square lattice by

$$n_x \cong 0.2 \left(\frac{4R}{v_0}\right)^{\frac{i}{i+2}} \exp\left(\frac{1}{(i+2)kT}(iE_m + E_i)\right) . \tag{1}$$

k is the Boltzmann constant and E_i the binding energy of the critical nucleus, i.e. $E_0 = E_1 = 0$, $E_2 = E_b$ and $E_3 \cong 2E_b$. This is one of the simplest approximations where E_i is given by the number of nearest neighbor adatom bonds in the critical nucleus i times the binding energy E_b.

Figure 2 shows the measured temperature dependence of the saturation island density at a coverage of 0.1 ML and a flux of 1.34×10^{-3} ML/s. Between

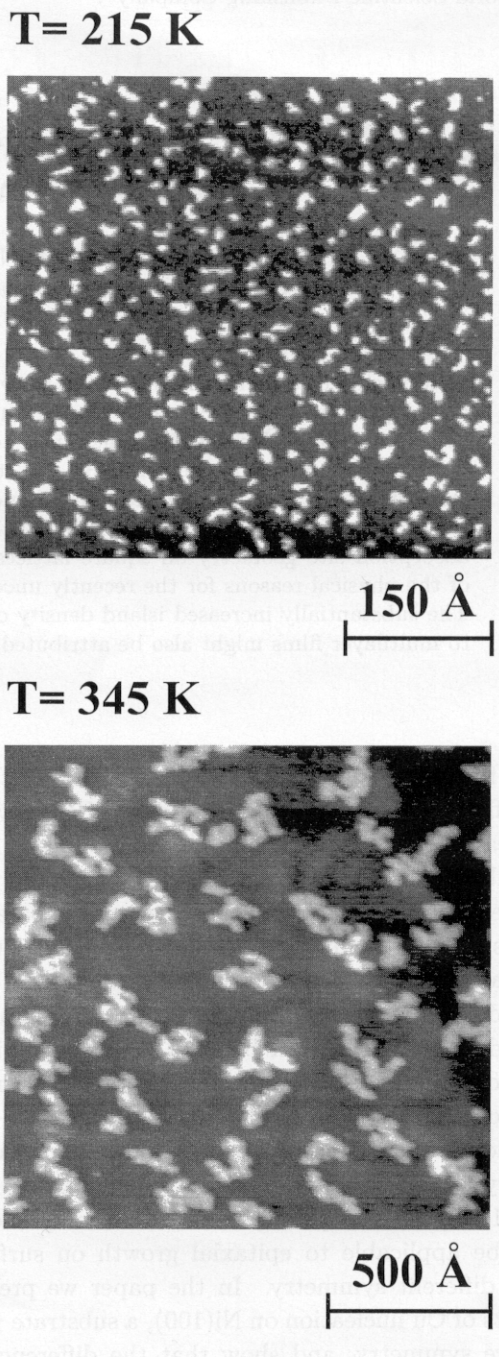

Fig. 1. STM images characterizing the saturation island density of Cu on Ni(100) at different growth temperatures. The deposition rate was 1.34×10^{-3} ML/s and the coverage corresponds to 0.1 ML.

100 and 400 K, the island density and the mean island size vary over three-and-a-half orders of magnitude. One can clearly distinguish between three regions which differ in slope. Below 160 K the island

density does not vary with temperature, indicating statistical growth with $i = 0$. Simulations by means of rate equations reveal, however, that the dimer is still the smallest stable island in this regime, but that a nonnegligible monomer concentration is present after deposition. Consequently, the island density and the island size distribution change by postgrowth and postnucleation through incorporation of monomers after deposition.[5] Above 160 K the saturation island density drops with increasing temperature, showing a pronounced break in the slope at 320 K, indicating a transition in critical size from $i = 1$ to $i = 3$. The assignment of the critical island sizes has been proven by the rate dependency of the saturation island density $n_x(R)$.[5] The two diffusion parameters for monomer migration, E_m and ν_0, are obtained in the temperature range between 160 and 320 K, where $i = 1$. The slope of the linear fit results in a migration barrier of (0.351 ± 0.017) eV. The related value of the attempt frequency corresponds to $4 \times 10^{(11 \pm 0.3)}$ Hz. The dimer bond energy is found by the slope of the linear fit where $i = 3$ and yields a value of (0.46 ± 0.19) eV. The attempt frequency, $5 \times 10^{(12 \pm 2)}$ Hz, corresponds to the attempt frequency of the $i = 1$ case within the error bars. It is interesting to note that a similar migration barrier, $E_m = (0.36 \pm 0.03)$ eV, has been measured for the homoepitaxial Cu/Cu(100) system.[6] Simulations using molecular dynamics/Monte Carlo corrected effective medium theory (MD/MC-CEM) yield higher values for Cu/Ni(100), 0.62 eV[7] and 0.45 eV,[8] respectively, which crucially depend on the assumed rigidity of the substrate. The latter value is consistent with effective medium calculations using the EMT code of Stoltze and coworkers,[9] yielding $E_m = 0.47$ eV for Cu/Ni(100) with substrate relaxation. EMT seems to slightly overestimate migration barriers for hopping diffusion on square lattices.

The dimer bond energy of $E_b = (0.46 \pm 0.19)$ eV is surprisingly large. Our value for Cu/Ni(100) is one order of magnitude larger than that estimated for Cu/Cu(100).[6] EMT calculations,[9] however, yield an activation barrier for dimer dissociation of 0.74 eV and, therefore, the dimer bond energy, which is the difference between dimer dissociation and migration barrier, corresponds to 0.27 eV, which is in reasonable agreement with our result. The large dimer bond energy with respect to the migration barrier is responsible for the well-defined transition from $i = 1$ to $i = 3$ for Cu/Ni(100). On the basis of kinetic Monte Carlo simulations, Bartelt *et al.*[10] recently showed for homoepitaxy that a direct transition from $i = 1$ to a well-defined $i = 3$ regime is predicted if $E_b \geq E_m$, which is experimentally verified for Cu/Ni(100) in the present study.

The strong Cu–Cu bonding on Ni(100) is expected to be of importance for the recently found strain-relieving mechanism in Cu multilayers on

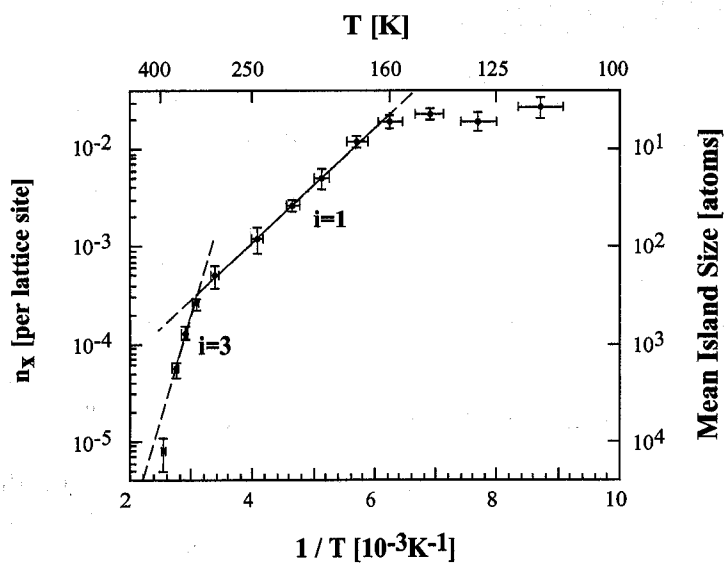

Fig. 2. Arrhenius plot of the saturation island density for Cu/Ni(100) (flux 1.34×10^{-3} ML/s; coverage 0.1 ML).

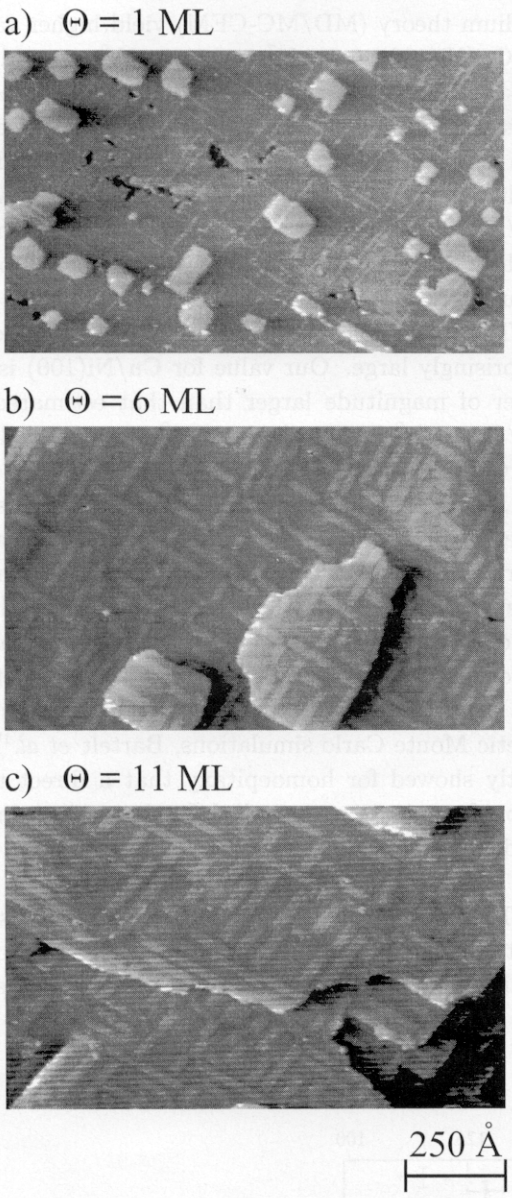

Fig. 3. STM images obtained characterizing the multilayer films of copper on Ni(100) (substrate temperature 345 K, flux 1.34×10^{-3} ML/s).

Ni(100) (−2.6% compressive strain) — the *internal {111} faceting.*[11] This mechanism is associated with the formation and growth of stripe patterns in the Cu multilayers, as shown in Fig. 3. These stripes have a height Δh of about 0.5 Å (step height 1.8 Å),[11,12] independent of coverage. The width of the stripes D, however, grows stepwise with coverage up to about 20 ML; see Fig. 3. For monolayer coverage, the stripes are exactly one atom wide, for 2 ML two atoms and so on. The other parameters, like the stripe density, the length distribution and the mean length, stay constant.[13] Thus, the patterns formed in the first monolayer are stabilized by the creation of internal {111} facets along the stripes in the multilayer films (cp. model in Fig. 4).

The internal faceting model fully accounts for these experimental observations. It is motivated by the fact that the compressive strain at fcc(100) is highest in close-packed ⟨110⟩ directions. Therefore, chains of atoms are squeezed out from the adlayer and create protruding stripes. Due to the square symmetry, these stripes are formed in both ⟨110⟩ directions, perpendicular and parallel to the substrate step edges. The simplest way to generate such stripes is to shift Cu atoms from fourfold hollow to twofold bridge sites (see Fig. 4; coverage 1 ML). Bridge site atoms have a reduced number of nearest neighbors in the substrate layer but gain binding energy in the copper film. There are two nearest neighbors below and, in addition, four lateral neighbors with a binding length which is only about 10% larger.

Due to the large lateral Cu bond strength the total lowering of the binding energy will be low. On the other hand, the copper film can (partially) relieve its strain due to the gain of lateral freedom of expansion. Obviously, this lateral freedom of expansion is overbalancing the lowered binding energy.

The exceptional strong Cu–Cu interaction on Ni(100) is also the reason for the increased island density on top of the first and the second copper monolayer (see Fig. 3), compared with the island densities on Cu multilayers. With increasing film thickness the film adopts copper-like behavior, i.e. finally the nucleation kinetics will resemble those of Cu(100). As the diffusion barriers for Cu on Cu(100) and Ni(100) are similar but the dimer bond energy deviates substantially, this difference is the origin of the different island densities in the monolayer and at the multilayers. Indeed, assuming $i = 3$ and similar E_m values a binding energy difference of a factor of 10 results in a difference in island densities of more than two orders of magnitude [Eq. (1)], in fair agreement with the observation in Fig. 3. Above 2 ML coverage we have only found flat terraces at 345 K. This observation is also supported by high resolution LEED measurements during epitaxial growth.[12] The peak intensity shows two oscillations related to the growth of the first and the second monolayer and, above 2 ML, it decreases monotonously due to the increase of the surface covered by stripes. Above bilayer coverage

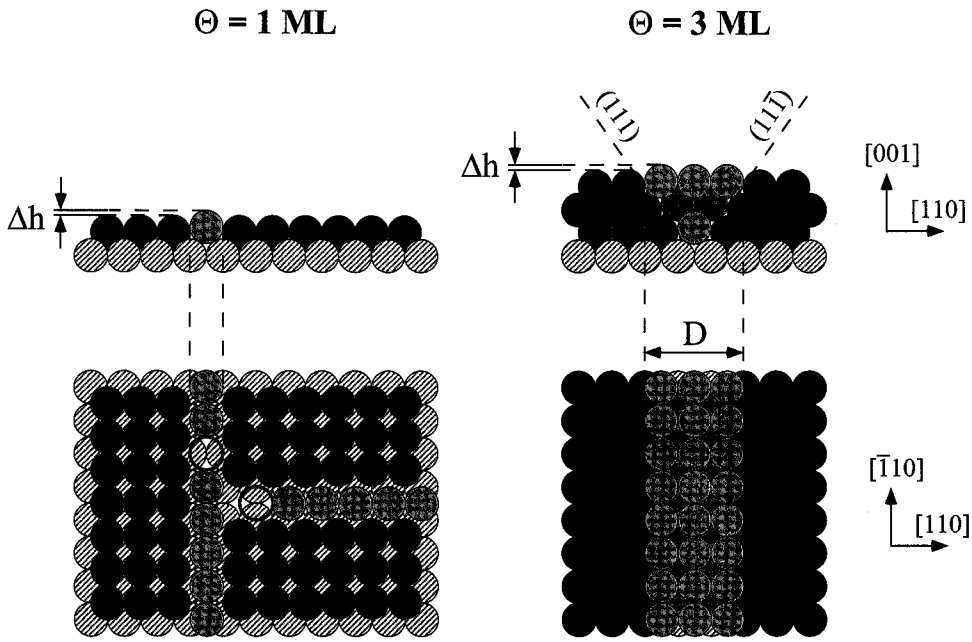

Fig. 4. Internal faceting model describing the formation and growth of the stripe pattern as a strain-relieving mechanism in Cu heteroepitaxy on Ni(100).

the oscillations disappear, since the film grows in step flow mode at 345 K.

Acknowledgments

The support of the Alexander von Humboldt-Stiftung (B. M.) and the Deutscher Akademischer Austauschdienst (L. N.) is gratefully acknowledged.

References

1. J. A. Venables, G. D. T. Spiller and M. Hanbücken, *Rep. Prog. Phys.* **47**, 399 (1984).
2. H. Brune, H. Röder, K. Bromann and K. Kern, *Phys. Rev. Lett.* **73**, 1955 (1994).
3. J.-K. Zuo, J. F. Wendelken, H. Dürr and C.-L. Liu, *Phys. Rev. Lett.* **72**, 3064 (1994).
4. H. Brune, H. Röder, C. Boragno and K. Kern, *Thin Solid Films* **264**, 230 (1995).
5. B. Müller, L. Nedelmann, B. Fischer, H. Brune and K. Kern, submitted to *Phys. Rev. B.*
6. H. Dürr, J. F. Wendelken and J.-K. Zou, *Surf. Sci.* **328**, L527 (1995).
7. D. E. Sanders and A. E. DePristo, *Surf. Sci.* **260**, 116 (1992).
8. L. S. Perkins and A. E. DePristo, *Surf. Sci.* **319**, 225 (1994).
9. P. Stoltze, *J. Phys.: Condens. Matter* **6**, 9495 (1994).
10. M. C. Bartelt, L. S. Perkins and J. W. Evans, *Surf. Sci.* **344**, L1193 (1995).
11. B. Müller, B. Fischer, L. Nedelmann, A. Fricke and K. Kern, *Phys. Rev. Lett.* **76**, 2358 (1996).
12. L. Nedelmann, B. Müller, B. Fischer, K. Kern, D. Erdös, J. Wollschläger and M. Henzler, submitted to *Surf. Sci.*
13. B. Müller, L. Nedelmann, B. Fischer, A. Fricke and K. Kern, *J. Vac. Sci. Technol.* **A14** (1996).